

Analysis of Diffusion Based Molecular Communication System with Multiple Transmitters

Nithin V. Sabu and Abhishek K. Gupta

Abstract

Due to the limited capabilities of a single bio-nanomachine, complicated tasks can be performed only with the co-operation of multiple bio-nanomachines. In this work, we consider a diffusion-based molecular communication system with a transmitter bio-nanomachine (TBN) communicating with a fully-absorbing spherical receiver bio-nanomachine (RBN) in the presence of other TBNs. The bits transmitted by each of the TBNs are considered as random in each time slot and different for each TBNs in contrary to the past works in literature with deterministic bits, which are same to all TBNs. The TBNs are modeled using a marked Poisson point process (PPP) with the location of TBNs as points of PPP, and the transmit bits as marks. In this paper, we derive the expected number of molecules observed at the RBN and the bit error probability of the system. We validate our analysis using numerical results and provide various design insights about the system.

I. INTRODUCTION

Molecular communication can enable bio-nanomachines (biological devices with nanoscale functional units) to communicate with each other by sending and receiving messenger molecules termed as *information molecules* (IMs). The transmitter bio-nanomachine (TBN) first encodes the transmit message into IMs [2]. Then, the TBN emits IMs to the propagation medium, and the IMs propagate to the receiver bio-nanomachine (RBN). In molecular communication via diffusion (MCvD) systems, the propagation is due to diffusion via Brownian motion [3]. The

The authors are with the department of Electrical Engineering, Indian Institute of Technology Kanpur, Kanpur, India 208016. (Email: nithinvs@iitk.ac.in and gkrabhi@iitk.ac.in). This research was supported by the Science and Engineering Research Board (DST, India) under the grant SRG/2019/001459. A part of the paper will appear in [1].

receptors present on the surface of the RBNs bind the IMs, and RBNs do further processing to estimate the transmitted information.

The channel model for a three dimensional (3D) MCvD system with a point TBN and a fully-absorbing receiver (absorbs all the IMs hitting its surface) was derived in [4]. The IMs of the same type emitted from the interfering TBNs also propagates to the receiver to cause multi-transmitter interference (MTI) [5]. In literature, the spatial distribution of bacterial colonies inside cheese was shown to follow the Poisson point process PPP [6]. Therefore, the location of the bio-nanomachines in the 3D space can be modeled using PPP. The expected number of molecules absorbed at the passive and fully-absorbing spherical receivers, when the TBNs are distributed as PPP was derived in [7]. The authors also derived the probability of bit error for the same system. The work [8] derived the expected number of molecules received at a fully-absorbing receiver by considering both inter-symbol interference (ISI) and MTI when the number of interfering TBNs is constant. The analytical expression for the total signal strength and the bit error probability at the partially absorbing spherical receiver when the interfering transmitters are distributed as a PPP was derived in [9].

The expected absorbed molecules and the probability of bit error was calculated in the past works [7], [9], [10] by considering all the PPP distributed TBNs are sending the same bit sequence. In an MCvD with multiple TBNs, each TBN can have individual transmit data that may be distributed according to an arbitrary probability distribution over information symbols and can be independent of other TBNs. For such a system in practical scenarios, it is essential to include the independence and randomness of transmit data across TBNs in the system model. This was not studied in past works, which is the focus of this work.

In this work, we consider a 3D MCvD system with multiple interfering TBNs and a fully-absorbing spherical RBN. The location of the associated TBN is assumed to be fixed, or the associated TBN is the nearest transmitter. The interfering TBNs are modeled as a marked PPP (MPP) with their location as points of PPP and the transmit bits as marks. The transmit bits at each TBN is assumed to be random and independent of transmit bits at other TBNs. In this paper, we derive the expected number of IMs observed at the RBN and the probability of bit error of the system. We also discuss the relevance of accurately incorporating the randomness of the data to be transmitted.

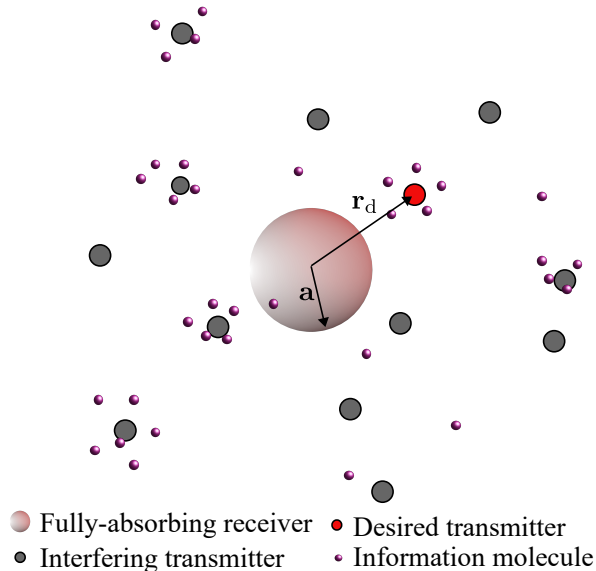


Fig. 1. System model. An MCvD system with a typical spherical fully absorbing RBN at the origin. The location of the desired TBN (\mathbf{x}_d , shown as red circle) can either be fixed or nearest to the RBN and the interfering TBNs (shown as grey circle) form a MPP.

II. SYSTEM MODEL

In this work, we consider an MCvD system in a 3D fluid medium without flow, with a fully absorbing spherical RBN and multiple TBNs, as shown in Fig. 1. The TBNs are assumed to be point sources, which emit IMs to the fluid medium based on on-off keying (OOK) modulation.

Network Model: Consider a typical fully-absorbing spherical RBN of radius a located at the origin. The whole surface of the RBN is covered with receptors that can bind only a single type of molecules. All the IMs reaching the surface of RBN are attached to the receptors and are counted for demodulation.

Assume that the TBN associated with the typical RBN, termed *tagged* TBN, is located at \mathbf{x}_d . We consider two cases; one with the tagged TBN at a fixed location and other with the nearest transmitter as the tagged TBN. The interfering TBN locations can be modeled using a 3D homogeneous PPP Φ [10]. Since the RBN occupies the space $\mathcal{B}(0, a)$ (ball of radius a centered at the origin), the support of PPP is taken as $\mathbb{R}^3 \setminus \mathcal{B}(0, a)$ [10]. The union of the location of the desired TBN and the interfering TBNs PPP (Φ) is denoted by $\{\mathbf{x}_d\} \cup \Phi$.

Modulation and transmission model: Consider the transmit bit of the TBN located at \mathbf{x} (denoted by $s_{\mathbf{x}}$), is assumed to be a Bernoulli RV with parameter p_1 . At the beginning of the

time slot (of duration T_S), the point TBN emits u_x number of molecules into the fluid medium. The modulation scheme we consider is OOK. Therefore $u_x = N$ when $s_x = 1$ and $u_x = 0$ otherwise. u_x can be 0 with probability $p_0 = 1 - p_1$ and N with probability p_1 . u_x can be considered as the mark of the TBN, and the interfering TBNs can be modeled using a marked PPP $\Phi_M = \{(\mathbf{x}, u_x) : \mathbf{x} \in \Phi\}$ [11]. Also, the TBNs and RBN are assumed to be synchronized in time.

Propagation model: Among various propagation mechanisms, we consider free diffusion for sending the IMs from TBN to RBN. The TBN emits the IMs to the propagation medium, and it moves to the RBN via 3D Brownian motion.

Channel and receiving model: Consider a TBN located at \mathbf{x}_t transmitting IMs to the propagation medium. The fraction of IMs observed at the RBN within time t since the transmission at time $t = 0$ be denoted by $f(t, \|\mathbf{x}_t\|)$. The fraction of IMs observed at the RBN during the time interval $[0, T_S]$ is

$$h_{\|\mathbf{x}_t\|} = f(T_S, \|\mathbf{x}_t\|). \quad (1)$$

$h_{\|\mathbf{x}_t\|}$ is also known as channel impulse response (CIR). Considering the event of observation of an IM at the RBN as a Bernoulli trial with probability of success $h_{\|\mathbf{x}_t\|}$, the number of molecules $y_{\mathbf{x}_t}$ observed at the RBN follows Binomial distribution with parameter $(N, h_{\|\mathbf{x}_t\|})$, where N is the number of transmitted IMs. We can approximate Binomial distribution with Poisson distribution for mathematical tractability when N is large and $h_{\|\mathbf{x}_t\|}$ is small. Hence $y_{\mathbf{x}_t} \sim \mathcal{P}(Nh_{\|\mathbf{x}_t\|})$. The total number of desired IMs reaching the RBN due to the emission of IMs from the tagged TBN is

$$y_S \sim \mathcal{P}(h_{\|\mathbf{x}_d\|} u_{\mathbf{x}_d}). \quad (2)$$

Similarly, the total number of MTI molecules reaching the RBN due to the emission of IMs from the interfering TBNs, given Φ , is

$$y_M \sim \mathcal{P}\left(\sum_{\mathbf{x}_t \in \Phi} h_{\|\mathbf{x}_t\|} u_{\mathbf{x}_t}\right). \quad (3)$$

Therefore, the total number of molecules absorbed by the RBN at any time slot is the sum of the desired molecules and MTI molecules.

Decoding at the RBN: We consider a threshold detector at the RBN to demodulate the transmitted information. The RBN counts the total number of IMs absorbed (y) in a time slot,

and at the end of the time slot, y is compared with a predefined threshold η . The bit s_{x_d} transmitted from the tagged TBN is estimated as $\hat{s}_{x_d} = 0$ if $y < \eta$, otherwise $\hat{s}_{x_d} = 1$. Due to the diffusion of IMs and due to the presence of interfering TBNs in the propagation medium, errors can occur in the demodulation process. An error would occur at the RBN when the transmitted bit $s_{x_d} = 0$ is decoded as $\hat{s}_{x_d} = 1$ and vice versa. Therefore, the total probability of bit error (P_e) at any time slot is given by

$$P_e = p_0 P_{e0} + p_1 P_{e1} \quad (4)$$

where P_{e0} and P_{e1} are the probability of incorrect decoding for bit 0 and 1 formally defined as $P_{e0} = \mathbb{P}[\hat{s}_{x_d} = 1 | s_{x_d} = 0]$ and $P_{e1} = \mathbb{P}[\hat{s}_{x_d} = 0 | s_{x_d} = 1]$.

Modeling molecular degradation: The performance of a MCvD can be improved by incorporating adequate degradation of IMs in the design. IMs degrade over time due to the reaction with other molecules existing or added intentionally in the propagation medium. We consider exponential degradation, where the probability that an IM will degrade only after time t is equal to $\exp(-\mu t)$. Here, μ denotes the reaction rate constant, and μ is related to the half-time ($\Lambda_{1/2}$) as $\mu = \ln(2)/\Lambda_{1/2}$. $\mu \rightarrow 0$ (*i.e.* $\Lambda_{1/2} \rightarrow \infty$) corresponds to IM with no degradation.

We assume that the considered molecular communication system does not have inter symbol interference. Some examples of such systems include cases where the symbol time T_S is sufficiently large and/or molecular degradation rate is sufficient.

Channel impulse response: The hitting rate of molecules at the surface of the RBN (*i.e.* total number of molecules hitting the RBN in unit time) at time τ , due to the emission of IMs from a point TBN located r distance away from the center of RBN is given as [4],

$$\kappa(\tau, r) = \frac{a}{r} \frac{r-a}{\sqrt{4\pi D\tau^3}} \exp\left(-\frac{(r-a)^2}{4D\tau}\right), \quad (5)$$

where D represents the diffusion coefficient, which depends on the properties of IM and the propagation medium. The fraction of non-degraded IMs observed at the RBN within time t , is given by [12],

$$f(t, r) = \int_0^t \kappa(\tau, r) \times \exp(-\mu\tau) d\tau \quad (6)$$

$$= \frac{a}{2r} \left[\exp\left(-\sqrt{\frac{\mu}{D}}(r-a)\right) \operatorname{erfc}\left\{\frac{r-a}{\sqrt{4Dt}} - \sqrt{\mu t}\right\} + \exp\left(\sqrt{\frac{\mu}{D}}(r-a)\right) \operatorname{erfc}\left\{\frac{r-a}{\sqrt{4Dt}} + \sqrt{\mu t}\right\} \right]. \quad (7)$$

Observations at the RBN: The total number of IMs arriving at the RBN due to the emission of IMs from the tagged and interfering TBNs is $y = y_S + y_M$. Using (2), (3), and since the sum of Poisson random variables is also Poisson random variable, $y \sim \mathcal{P} \left(\sum_{\mathbf{x}_t \in \Phi_T} h_{\|\mathbf{x}_t\|} u_{\mathbf{x}_t} \right)$. From (2), the expected number of desired IMs observed at the RBN is

$$E_S = \mathbb{E} [y_S] = p_1 N f(T_S, r_d). \quad (8)$$

The expected number of molecules arriving at the RBN due to MTI is

$$E_M = \mathbb{E} [y_M] = \mathbb{E} \left[\sum_{\mathbf{x} \in \Phi} h_{\|\mathbf{x}\|} u_{\mathbf{x}} \right]. \quad (9)$$

Applying Campbell Mecke theorem [13] in (9) gives,

$$\begin{aligned} E_M &= 4\pi\lambda \int_a^\infty h_z \mathbb{E}[u_z] z^2 dz \\ &= 4\pi\lambda p_1 N \int_a^\infty f(T_S, z) z^2 dz. \end{aligned}$$

Now from (8) and (9), the expected total number of IMs absorbed by the RBN ($E_T = E_S + E_M$) at any time slot is

$$E_T = p_1 N \left(f(T_S, r_d) + 4\pi\lambda \int_a^\infty f(T_S, z) z^2 dz \right). \quad (10)$$

Special case: When $T_S \rightarrow \infty$,

$$E_M = 4\pi\lambda p_1 N a \left(\frac{D}{\mu} + a \sqrt{\frac{D}{\mu}} \right). \quad (11)$$

In (11), when $T_S \rightarrow \infty$, the expected number of observed molecules due to MTI increases with λ, p_1, N, a and D , and decreases with μ . Also in (11), we can see that when $\mu \rightarrow 0$ (no molecular degradation), $E_M \rightarrow \infty$. This implies that, for a system with IM does not degrade over time, the expected MTI molecules will tend to infinity when $T_S \rightarrow \infty$.

III. PROBABILITY OF BIT ERROR

The probability of bit error as defined in (4) for the considered MCvD system is derived in this section. First, we consider the distance r_d between the tagged TBN and the RBN is fixed, and we derive the P_e . We then obtain P_e when the desired transmitter is the nearest TBN.

A. *When the tagged TBN is at a fixed distance:*

The probability of bit error for the case when r_d is fixed is given in Theorem 1.

Theorem 1. *When the tagged TBN is at a fixed distance from the RBN, the probability of bit error is given by (4) with the probability of incorrect decoding of bit 0 and 1 given as*

$$P_{e0} = 1 - e^{-\alpha_0(\lambda)} \left[1 + \sum_{n=1}^{\eta-1} \frac{1}{n!} \mathfrak{B}_n(\boldsymbol{\alpha}(\lambda)) \right], \quad (12)$$

$$P_{e1} = e^{-\alpha_0(\lambda) - Nf(T_S, r_d)} \times \left[1 + \sum_{n=1}^{\eta-1} \frac{1}{n!} \mathfrak{B}_n(\boldsymbol{\beta}(r_d, \lambda)) \right], \quad (13)$$

where $\alpha_0(\lambda) = 4\pi\lambda p_1 \int_a^\infty [1 - e^{-Nf(T_S, z)}] z^2 dz$, $\boldsymbol{\alpha}(\lambda) = [\alpha_1(\lambda), \alpha_2(\lambda), \dots, \alpha_{\eta-1}(\lambda)]$ and $\boldsymbol{\beta}(r_d, \lambda) = [\alpha_1(\lambda) + Nf(T_S, r_d), \alpha_2(\lambda), \dots, \alpha_{\eta-1}(\lambda)]$ with

$$\alpha_i(\lambda) = 4\pi\lambda p_1 \int_a^\infty e^{-Nf(T_S, z)} (Nf(T_S, z))^i z^2 dz. \quad (14)$$

Here, $\mathfrak{B}_n(\cdot)$ denotes the n th complete exponential Bell polynomial [14] given as

$$\mathfrak{B}_n(\boldsymbol{\alpha}(\lambda)) = \sum_{w=1}^n \sum_{j_1! j_2! \dots j_{n-w+1}!} \frac{n!}{j_1! j_2! \dots j_{n-w+1}!} \prod_{v=1}^{n-w+1} \left(\frac{\alpha_v(\lambda)}{v!} \right)^{j_v}. \quad (15)$$

where the second sum is taken over all non-negative integers $j_1, j_2, \dots, j_{n-w+1}$ such that $j_1 + j_2 + \dots + j_{n-w+1} = w$ and $1j_1 + 2j_2 + \dots + (n-w+1)j_{n-w+1} = n$.

Proof: See Appendix A. ■

B. *When the tagged TBN is the nearest transmitter:*

Now, consider the case when the nearest transmitter is the tagged TBN. This case is more realistic as the tagged TBN location is not fixed. The probability density function of r_d is

$$g_{R_d}(r) = 4\pi\lambda r^2 \exp\left(-\frac{4}{3}\pi\lambda(r^3 - a^3)\right) \quad (16)$$

The probability of bit error for this case is given in Theorem 2. The proof is very similar to the proof of Theorem 1 and hence is omitted for brevity.

Theorem 2. *When the nearest TBN is selected as the tagged TBN, the probability of bit error is given by (4) with the probability of incorrect decoding for bit 0 and 1 given as*

$$P_{e0} = 1 - e^{-\alpha_0(\lambda)} \left[1 + \sum_{n=1}^{\eta-1} \frac{1}{n!} \mathfrak{B}_n(\boldsymbol{\alpha}(\lambda)) \right], \quad (17)$$

$$P_{e1} = 4\pi\lambda e^{-\alpha_0(\lambda) + \frac{4}{3}\pi\lambda a^3} \int_a^\infty \left[1 + \sum_{n=1}^{\eta-1} \frac{1}{n!} \mathfrak{B}_n(\boldsymbol{\beta}(r_d, \lambda)) \right] \times \exp\left(-Nf(T_S, r_d) - \frac{4}{3}\pi\lambda r_d^3\right) r_d^2 dr_d \quad (18)$$

where $\alpha_0(\lambda)$, $\boldsymbol{\alpha}(\lambda)$ and $\boldsymbol{\beta}(r_d, \lambda)$ are the same as in Theorem 1.

IV. NUMERICAL RESULTS

In this section, the analytical expressions derived in the previous sections are validated using Monte Carlo based simulations, and several design insights about the system are discussed with the help of numerical results.

For the Monte Carlo simulation, the interfering TBNs are generated as PPP outside the RBN and up to a distance of $150\mu m$ from the center of the RBN. The simulation is carried out for 10^4 realizations of PPP. The interfering TBN density chosen for simulations is 10^{-5} TBNs per μm^3 , which corresponds to 141 interfering transmitters. For all simulations, the diffusion coefficient is fixed as $D = 74.9 \mu m^2/s$, fully-absorbing spherical receiver radius is fixed as $a = 4\mu m$, the number of molecules emitted for bit-1 is $N = 100$ molecules, degradation rate constant $\mu = 5s^{-1}$, and the duration of the time slot is set as 0.5s. The chosen value of μ and T_S ensure that the ISI is negligible. In all figures, solid lines represents the curves corresponding to the derived analytical expressions, and markers represent the simulation results unless otherwise mentioned.

Variation of E_S , E_M and E_T with the distance between the tagged TBN and the RBN (r_d):

The variation of E_S , E_M , and E_T with the distance between the surface of the spherical RBN and the tagged TBN (*i.e.*, $r_d - a$) can be seen in Fig. 2. The observation of the expected number of absorbed MTI molecules (E_M) at the RBN is independent of r_d . The tagged TBN location affects the number of desired IMs absorbed at the RBN (E_S). E_S and E_T decreases as the tagged TBN moves away from the RBN. When the tagged TBN moves far away from the RBN, E_S reduces to zero, and E_T is only due to E_M , which results in bit error and loss of information.

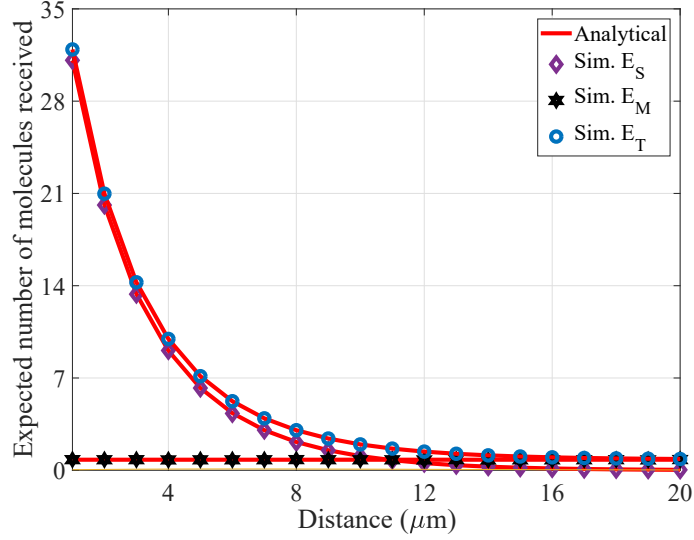


Fig. 2. Variation of the expected number of desired (E_S), MTI (E_M) and total (E_T) molecules absorbed at the receiver for a system with molecular degradation versus the distance between tagged TBN and the RBN's surface ($r_d - a$). Here, $\lambda = 1 \times 10^{-5}$ TBNs/ μm^3 .

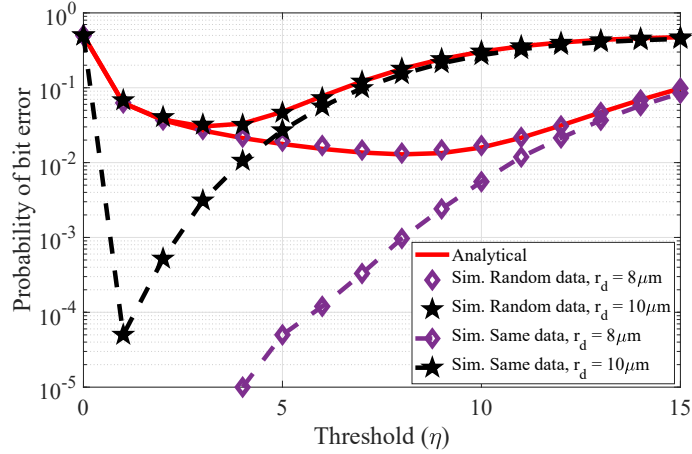


Fig. 3. Probability of bit error (P_e) versus threshold (η) when r_d is fixed. When r_d increases, P_e increases while the optimal threshold η_{opt} decreases.

Since E_T varies with r_d , the decoding threshold η at the RBN should be chosen according to r_d .

Impact of decoding threshold (η) on the probability of bit error (P_e) when the location of tagged TBN is fixed: Fig. 3 shows the variation of P_e with the threshold η when the tagged TBN location is fixed. Analytical results when transmit bits are random and different for each

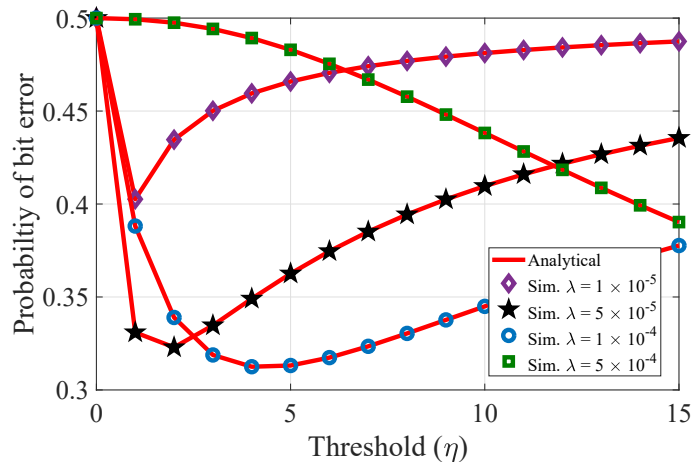


Fig. 4. Probability of bit error versus the threshold η with different interfering transmitter densities. Here, the tagged TBN is the nearest transmitter.

TBN (as derived in Theorem 1) are compared with corresponding simulation results for various values of r_d . As the threshold for detection increases, the probability of bit error P_e increases after it is first reduced to a minimum value. This behavior proves the existence of an optimum threshold η_{opt} for which P_e is minimum. When r_d increases, E_T reduces due to the reduction in E_S , and as a result, η_{opt} decreases. The probability of bit error at the optimum threshold increases with r_d due to the relative reduction in E_S in comparison to E_M .

Impact of accurately characterizing randomness and independence of transmit data across TBNs: In Fig. 3 we can observe that, considering transmit bits same for all TBNs as in previous works give inaccurate results (especially at low η values) compared to real scenarios (bits are random and different for TBNs).

Impact of decoding threshold (η) on the probability of bit error (P_e) when the tagged TBN is the nearest TBN: Fig. 4 shows the variation of P_e with the detection threshold for different TBN densities. Similar to Fig. 3, as η increases, P_e first decreases and achieves a minimum value and after that, P_e increases. We can observe that, when TBN density increases, the minimum probability of bit error reduces. This is because the nearest TBN is the desired transmitter, and when the TBN density increases, the desired transmitter comes closer to the receiver, and more signal molecules reach the receiver. Also, with the increase in TBN density, the optimal threshold η_{opt} increases due to more signal molecules reaching the receiver.

V. CONCLUSIONS

In this paper, we have presented an analytical framework for a 3D MCvD system with multiple point TBNs and a single fully-absorbing spherical RBN. The data transmitted by each TBNs are random independent of other TBNs. The analytical expressions for the expected number of signal and MTI molecules absorbed by the RBN were derived. We have also derived the analytical expressions for the probability of bit error under two scenarios; when the desired TBN is at a fixed location, and the desired TBN is the nearest transmitter. The necessity of incorporating the transmission data randomness and independence is also included in the discussion. As future work, we can consider the impact of leftover molecules from previous symbols (which can occur when the symbol duration is small and/or degradation of IMs is not adequate) along with MTI on the system performance.

APPENDIX A

PROOF OF THEOREM-1

Consider the bit to be transmitted by the tagged TBN in a time slot as b . Hence, $u_{\mathbf{x}_d} = bN$.

Let $v(\|\mathbf{x}\|)$ be the expected number of IMs absorbed by the RBN, that were emitted by the transmitter located at \mathbf{x} *i.e.*, $v(\|\mathbf{x}\|) = h_{\|\mathbf{x}\|}u_{\mathbf{x}}$. Let V be the expected total number of received molecules conditioned on Φ_M *i.e.*, $V(r_d, b, \Phi_M) = bNh_{r_d} + \sum_{\mathbf{x} \in \Phi_M} v(\|\mathbf{x}\|)$. Given Φ_M , the total number of IMs absorbed at the TBN is Poisson distributed *i.e.* $y \mid \Phi_M \sim \mathcal{P}(V(r_d, b, \Phi_M))$. Therefore, the probability of incorrect decoding for bit b is $P_{\text{eb}} = \mathbb{P}[y \notin [\tau_{\text{Lb}}, \tau_{\text{Hb}}]]$, where τ_{Hb} and τ_{Lb} are upper and lower threshold value of bit b . Here, $\tau_{\text{H0}} = \eta - 1$, $\tau_{\text{L0}} = 0$, $\tau_{\text{H1}} = \infty$, and $\tau_{\text{L1}} = \eta$. Now, the probability of incorrect decoding for bit b is given as

$$\begin{aligned} P_{\text{eb}} &= 1 - \sum_{n=\tau_{\text{Lb}}}^{\tau_{\text{Hb}}} \mathbb{E}_{\Phi_M} [\mathbb{P}[y = n \mid \Phi_M]] \\ &= 1 - \sum_{n=\tau_{\text{Lb}}}^{\tau_{\text{Hb}}} \mathbb{E}_{\Phi_M} \left[\frac{1}{n!} \exp(-V(r_d, b, \Phi_M)) \times V(r_d, b, \Phi_M)^n \right]. \end{aligned} \quad (19)$$

Note that, $\mathbb{E}[Z^n e^{-Z}] = (-1)^n \left. \frac{d^n \mathcal{L}_Z(\rho)}{d\rho^n} \right|_{\rho=1}$.

Applying this identity in (19), we get

$$P_{\text{eb}} = 1 - \sum_{n=\tau_{\text{Lb}}}^{\tau_{\text{Hb}}} \frac{1}{n!} (-1)^n \left. \frac{d^n \mathcal{L}_{V(r_d, b, \Phi_M)}(\rho)}{d\rho^n} \right|_{\rho=1}, \quad (20)$$

with the slight abuse of notation that $\frac{\partial^n F}{\partial \rho^n} = F$ for $n = 0$. In (20), $\mathcal{L}_V(\rho)$ is the Laplace transform of V which can be obtained as,

$$\begin{aligned} \mathcal{L}_{V(r_d, \mathbf{b}, \Phi_M)}(\rho) &= \mathbb{E} \left[\exp \left(-\rho \mathbf{b} N h_{r_d} - \rho \sum_{\mathbf{x} \in \Phi_M} v(\|\mathbf{x}\|) \right) \right] \\ &= \exp(-\rho \mathbf{b} N h_{r_d}) \mathbb{E}_{\Phi_M} \left[\exp \left(-\rho \sum_{\mathbf{x} \in \Phi_M} v(\|\mathbf{x}\|) \right) \right] \\ &\stackrel{(a)}{=} \exp \left(-\rho \mathbf{b} N h_{r_d} - 4\pi \lambda \int_a^\infty (1 - \mathbb{E}_{u_z} [e^{-\rho h_z u_z}]) z^2 dz \right) \\ &= \exp \left(-\rho N \mathbf{b} h_{r_d} - 4\pi \lambda p_1 \int_a^\infty (1 - e^{-\rho h_z N}) z^2 dz \right), \end{aligned} \quad (21)$$

where (a) is due to the marked version of Campbell theorem. By taking the n th derivative of (21) using the Bell polynomial version of Faa di Bruno's formula [14, eq.(2.2)], we get

$$\left. \frac{d^n \mathcal{L}_V(\rho)}{d\rho^n} \right|_{\rho=1} = \mathfrak{B}_n(\mathbf{P}(r_d, \lambda)) \times (-1)^n \exp \left(-\rho \mathbf{b} N h_{r_d} - 4\pi \lambda p_1 \int_a^\infty (1 - \exp(-h_z N)) z^2 dz \right), \quad (22)$$

where $\mathbf{P}(r_d, \lambda) = [P_1(r_d, \lambda), P_2(r_d, \lambda), \dots, P_{\eta-1}(r_d, \lambda)]$ with $P_m(r_d, \lambda) = N \mathbf{b} h_{r_d} \mathbb{1}(m = 1) + 4\pi \lambda p_1 \int_a^\infty e^{-h_z N} (h_z N)^m z^2 dz$. Now, substitute (22) in (20) with $\mathbf{b} = 0$ and $\mathbf{b} = 1$, we get (12) and (13) respectively.

REFERENCES

- [1] N. V. Sabu and A. K. Gupta, "Analysis of diffusion based molecular communication with multiple transmitters having individual random information bits," *IEEE Trans. Mol. Biol. Multi-Scale Commun. (to appear)*, pp. 1–1, 2020.
- [2] T. Nakano, A. W. Eckford, and T. Haraguchi, *Molecular communication*. Cambridge University Press, 2013.
- [3] A. Einstein, *Investigations on the theory of the brownian movement*. Courier Corporation, 1956.
- [4] H. B. Yilmaz, A. C. Heren, T. Tugcu, and C.-B. Chae, "Three-dimensional channel characteristics for molecular communications with an absorbing receiver," *IEEE Commun. Lett.*, vol. 18, no. 6, pp. 929–932, 2014.
- [5] M. Pierobon and I. F. Akyildiz, "Intersymbol and co-channel interference in diffusion-based molecular communication," in *Proc. ICC, IEEE*, 2012, pp. 6126–6131.
- [6] S. Jeanson, J. Chadœuf, M. N. Madec, S. Aly, J. Flourey, T. F. Brocklehurst, and S. Lortal, "Spatial distribution of bacterial colonies in a model cheese," *Applied and Environmental Microbiology*, vol. 77, no. 4, pp. 1493–1500, 2011.
- [7] Y. Deng, A. Noel, W. Guo, A. Nallanathan, and M. El-kashlan, "Analyzing large-scale multiuser molecular communication via 3-D stochastic geometry," *IEEE Trans. Mol. Biol. Multi-Scale Commun.*, vol. 3, no. 2, pp. 118–133, 2017.
- [8] E. Dinc and O. B. Akan, "Theoretical limits on multiuser molecular communication in internet of nano-bio things," *IEEE Trans. Nanobiosci.*, vol. 16, no. 4, pp. 266–270, 2017.
- [9] M. B. Dissanayake, Y. Deng, A. Nallanathan, M. El-kashlan, and U. Mitra, "Enhancing the reliability of large-scale multiuser molecular communication systems," in *Proc. SPAWC, IEEE*, 2018, pp. 1–5.
- [10] —, "Interference mitigation in large-scale multiuser molecular communication," *IEEE Trans. Commun.*, 2019.

- [11] J. G. Andrews, A. K. Gupta, and H. S. Dhillon, "A Primer on Cellular Network Analysis Using Stochastic Geometry," *arXiv preprint arXiv:1604.03183*, pp. 1–46, Apr 2016.
- [12] A. C. Heren, H. B. Yilmaz, C.-B. Chae, and T. Tugcu, "Effect of degradation in molecular communication: Impairment or enhancement?" *IEEE Trans. Mol. Biol. Multi-Scale Commun.*, vol. 1, no. 2, pp. 217–229, 2015.
- [13] M. Haenggi, *Stochastic geometry for wireless networks*. Cambridge University Press, 2012.
- [14] W. P. Johnson, "The curious history of Fa di Bruno's formula," *The American Mathematical Monthly*, vol. 109, no. 3, pp. 217–234, 2002.